Journal of Applied Sciences

ISSN 1812-5654

Journal of Applied Sciences 9 (6): 1147-1152, 2009
ISSN 1812-5654

Morphology and Thermal Stability of Chitosan and Methoxy Poly (ethylene glycol)-*b*-Poly (ϵ-caprolactone)/Poly(D, L-lactide) Nanocomposite Films

Supawut Khamhan and Yodthong Baimark
Center of Excellence for Innovation in Chemistry, Department of Chemistry
Faculty of Science, Mahasarakham University, Mahasarakham 44150, Thailand

Abstract: The objective of this study was to prepare biodegradable chitosan nanocomposite films contained dispersed nanoparticles of methoxy poly(ethylene glycol)-*b*-poly(ϵ-caprolactone) (MPEG-*b*-PCL) or methoxy poly(ethylene glycol)-*b*-poly(D,L-lactide) (MPEG-*b*-PDLL) diblock copolymers by solvent evaporation of nanoparticle suspension-chitosan solution. The nanoparticles were firstly produced in the chitosan solution by modified-spontaneous emulsification solvent diffusion method without any surfactants before film casting. The dispersed nanoparticles with approximately 100 and 300 nm in sizes for MPEG-*b*-PDLL and MPEG-*b*-PCL, respectively can be observed throughout the chitosan film matrices. Nanoparticle morphology was spherical shapes with smooth surfaces. The nanoparticles of MPEG-*b*-PDLL were smaller than the MPEG-*b*-PCL. The possible interactions between the chitosan film matrices and the nanoparticles were evaluated by thermogravimetry. Thermal stability of the chitosan film matrices were enhanced by nanoparticle incorporating. The chitosan/MPEG-*b*-PCL nanocomposite films had lower film transparency and moisture uptakes than the chitosan/MPEG-*b*-PDLL nanocomposite films. The both film transparency and moisture uptakes decreased as the diblock copolymer ratio increased.

Key words: Biodegradable films, nanoparticles, nanocomposite films, intermolecular bonding, thermogravimetry

INTRODUCTION

In recent years, increasing interest in biodegradable polymer films has developed mainly due to concern over the disposal of conventional synthetic polymers derived from petroleum. Conversely, biodegradable films from renewable sources not only are degraded readily after their disposal or implantation but also can extent the food shelf-life and the controlled release drug delivery, thus improving the quality of food and drug therapy, respectively. Among various available biodegradable polymers, considerable attention has been given to chitosan because of its unique properties.

The chitosan is a biopolymer that has received great attention in a variety of applications because of their biodegradability and biocompatibility (Ravi Kumaer *et al*., 2004; Muzzarelli and Muzzarelli, 2005). It is derived from chitin, which is the second most abundant polysaccharide on earth next to cellulose and is available from waste products in the shellfish industry. Because of its excellent film-forming property, chitosan can be used effectively as a film-forming material to carry active ingredients such as mineral or vitamin for food packaging applications (Park and Zhao, 2004; Rhim *et al*., 2006) and hydrophilic or hydrophobic drugs for drug delivery applications (Senel *et al*., 2000; Shu *et al*., 2001). The chitosan film does not promote prolonged drug release due to the fast dissolution rate in aqueous media. The hydrophobic drug-loaded poly(lactide-co-glycolide) microparticles have been incorporated into chitosan films to improve prolong drug release profiles (Perugini *et al*., 2003). However, these microcomposite films exhibit microphase separation, which may be give rise to inconsistent properties such as nanocomposite films.

Modified-spontaneous emulsification solvent diffusion method (modified-SESD method) has been used to prepare surfactant-free nanoparticles of hydrophilic-hydrophobic diblock copolymer (Baimark *et al*., 2007a). Higher energy apparatus, such as a homogenizer or a sonicator and surfactants were not used for this method.

In the earlier study by Baimark *et al*. (2007b) and Khamhan *et al*. (2008), the nanocomposite chitosan-based films containing methoxy poly (ethylene glycol)-*b*-poly (ϵ-caprolactone) diblock copolymer have been reported. The MPEG-*b*-PCL nanoparticles were formed in chitosan aqueous solution by the modified-spontaneous emulsification solvent diffusion method (modified-SESD method) before film casting. In this research, the nanocomposite chitosan-based films containing methoxy poly (ethylene glycol)-*b*-poly (D, L-lactide) diblock

---

Corresponding Author: Yodthong Baimark, Department of Chemistry, Faculty of Science, Mahasarakham University, Mahasarakham 44150, Thailand Tel: +66-43-754246 Fax: +66-43-754246

copolymer were prepared for comparison in morphology and thermal stability. The film transparency and moisture uptakes were also determined.

MATERIALS AND METHODS

Materials: Chitosan (90% deacetylation and molecular weight of 80 kDa) was purchased from Seafresh Chitosan Lab Co., Ltd., (Thailand) and used without further purification. Acetic acid (99.7%, Merck, Germany) was used as received. Methoxy poly(ethylene glycol)-*b*-poly (ϵ-caprolactone) (MPEG-*b*-PCL) and methoxy poly (ethylene glycol)-*b*-poly (D, L-lactide) (MPEG-*b*-PDLL) diblock copolymers were synthesized by using MPEG with molecular weight of 5,000 g mol^{-1} and stannous octoate as the initiating system as described in the earlier studies by Baimark *et al.* (2007a) and Baimark *et al.* (2007b).

Molecular weights of the MPEG-*b*-PCL and MPEG-*b*-PDLL obtained from curves of gel permeation chromatography were 62,300 and 73,600 g mol^{-1}, respectively.

Methods

Preparation of nanocomposite films: Nanoparticles of MPEG-*b*-PCL or MPEG-*b*-PDLL diblock copolymers were prepared by the modified-SESD method in chitosan solution without any surfactants. The chitosan solution was prepared by using 1% (v/v) acetic acid aqueous solution as the solvent. The preparation of nanocomposite films was typically described as follows. The diblock copolymer was dissolved in 2 mL of 4/1 (v/v) acetone/ethanol mixture. The diblock copolymer solution was then added drop-wise into 20 mL of chitosan solutions with stirring at 600 rpm. The organic solvent was removed in fume hood for 5 h. The nanoparticles suspended in the chitosan solution were obtained. Then, the film casting was done on Petri dish and subsequently dried at 30°C for 72 h. The nanocomposite films with chitosan/diblock copolymer ratios of 100/0, 90/10, 80/20 and 70/30 (w/w) were investigated. The resulted nanocomposite film was kept *in vacuo* at room temperature for a week before characterization.

Characterization of nanocomposite films: FT-IR spectroscopy was used to characterize functional groups of the both chitosan and diblock copolymer in nanocomposite films with air as the reference. The FT-IR spectra of films were obtained with resolution of 4 cm^{-1} and 32 scans.

Thermal stability of the films was determined by thermogravimetry (TG) using a TA-Instrument TG SDT Q600 thermogravimetric analyzer. For TG analysis, 10-20 mg sample was heated from 50 to 1,000°C at the heating rate of 20°C min^{-1} under nitrogen atmosphere.

Morphology of film surfaces and cross-sections was investigated by Scanning Electron Microscopy (SEM) using a JEOL JSM-6460LV SEM. The film cross-section was obtained after cutting film with paper-scissors. Before SEM measurement, the films were sputter coated with gold for enhancing the surface conductivity.

Film transparency was determined by UV-Vis spectroscopy using a Perkin-Elmer Lambda 25 UV-Visible spectrophotometer at 660 nm as described in the earlier studies by Khamhan *et al.* (2008).

Moisture uptake (%) of the chitosan and nanocomposite films was determined following the method. Briefly, the sample films with 20×20 mm in size were dried *in vacuo* at room temperature for a week. After weighing, they were kept in a desiccator with 90±5% relative humidity maintained with a saturated sodium chloride solution at 30±2°C. The sample films were weighed again after keeping in the close desiccator for 48 h. The moisture uptake (%) was calculated by Eq. 1.

$$\text{Moisture uptake (\%)} = (M_f - M_i)/M_i \times 100 \qquad (1)$$

where, M_i and M_f are the initial and final weight (g) of the films before and after moisture absorption test, respectively.

RESULTS AND DISCUSSION

FTIR analysis: The amine, residual amide and hydroxyl groups of chitosan can form the intermolecular hydrogen bonds with the ether and carbonyl groups in PEG and polylactide, respectively (Zhang *et al.*, 2002; Chen *et al.*, 2005). Existence of these intermolecular bonding were investigated from FTIR spectra. The FTIR spectrum of chitosan film in Fig. 1a shows the absorption bands at 1,654 and 1,587 cm^{-1} attributed to the amide carbonyl group (amide I) and the free amino groups, respectively. The FTIR spectrum of MPEG-*b*-PCL in Fig. 1e shows the strong carbonyl band at 1,724 cm^{-1} and CH stretching

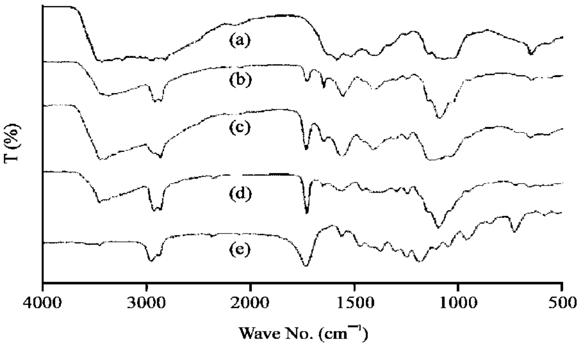

Fig. 1: FTIR spectra of (a) chitosan, (b) 90/10, (c) 80/20, (d) 70/30 (w/w) chitosan/MPEG-*b*-PCL nanocomposite and (e) MPEG-*b*-PCL films

vibration band at 2867 cm^{-1} of PCL and MPEG blocks, respectively. The FTIR spectra of chitosan/MPEG-*b*-PCL nanocomposite films are shown in Fig. 1b-d. These spectra demonstrated the both absorption bands characteristics of chitosan and MPEG-*b*-PCL. As would be expected, the intensities of carbonyl bands increased with the MPEG-*b*-PCL ratio. The FTIR spectra of chitosan/MPEG-*b*-PDLL nanocomposite films show similar evidence as the chitosan/MPEG-*b*-PCL nanocomposite films.

Film morphology: Film thicknesses of the chitosan and nanocomposite film measured from SEM images were in the ranges of 10-50 µm. The film thicknesses increased with the diblock copolymer ratio. Figure 2 and 3 shows SEM micrographs of film surfaces and cross-sections, respectively. The both surface and cross-section of chitosan film were smooth appearance as shown in Fig. 2a and 3a, respectively. While the incorporation of nanoparticles induced roughness on the both surfaces and cross-sections of the chitosan films.

The nanoparticles dispersed into chitosan films can be observed on the both film surfaces and cross-sections. The nanoparticles can be clearly detected on the film cross-sections. The nanoparticle morphology was spherical in shape with smooth surface (Fig. 3b, c). The

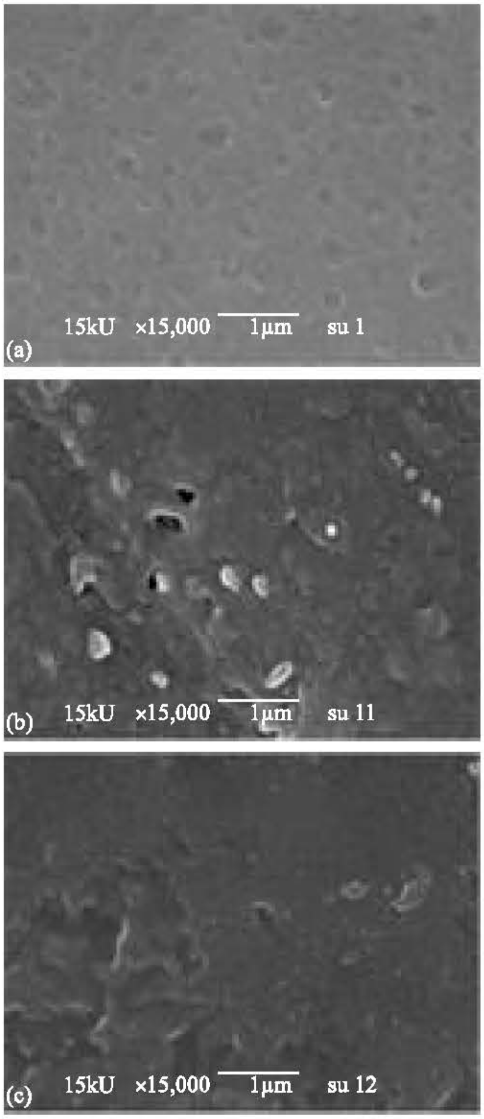

Fig. 2: SEM micrographs of film surfaces of (a) chitosan, (b) 70/30 (w/w) chitosan/MPEG-*b*-PCL nanocomposite and (c) 70/30 (w/w) chitosan/MPEG-*b*-PDLL nanocomposite (bar = 1 µm)

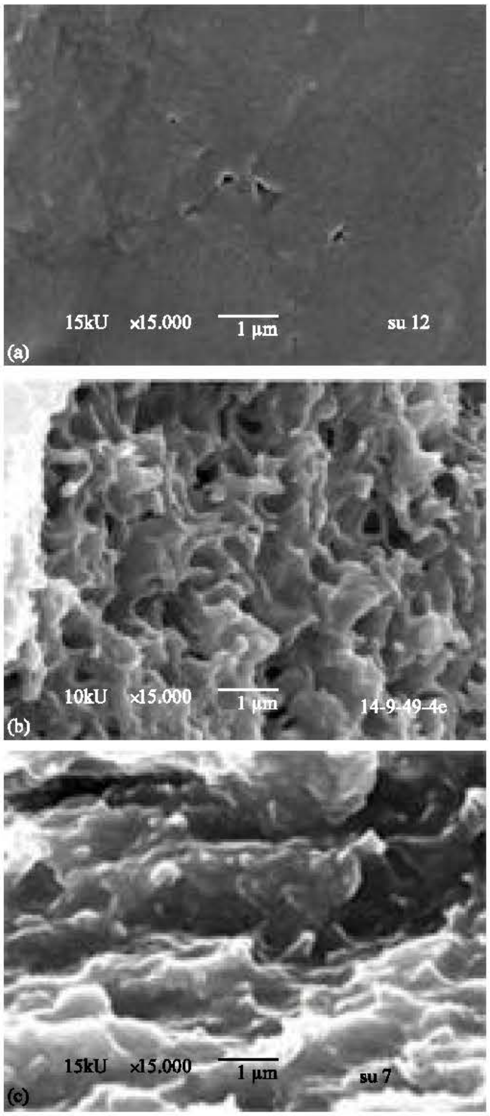

Fig. 3: SEM micrographs of film cross sections of (a) chitosan, (b) 70/30 (w/w) chitosan/MPEG-*b*-PCL nanocomposite and (c) 70/30 (w/w) chitosan/MPEG-*b*-PDLL nanocomposite (bar = 1 µm)

nanoparticle sizes of MPEG-*b*-PCL and MPEG-*b*-PDLL were approximately 200 and 100 nm, respectively. The number of the nanoparticles increased when the diblock copolymer ratio was increased. This may be expected that faster solidified rate of the MPEG-*b*-PCL nanoparticles after solvent diffusion process gave the larger size nanoparticles.

In addition, the nanopores were also observed on the film surfaces and cross-sections. This might be due to the nanoparticles were self-condensed and nano-scopically phase separated from the chitosan film matrices during the drying process. The film cross-section showed highly nanoporous structure than that observed at its surface. The interconnected nanopores were approximately 300 and 50 nm in sizes for the chitosan/MPEG-*b*-PCL and chitosan/MPEG-*b*-PDLL nanocomposite films, respectively, which indicates that these nanocomposite films contain nanoporous structures.

Thermal stability: Thermal stability of chitosan film and nanocomposite films was studied by TG analysis, which can be clearly determined from differential TG (DTG) thermograms as shown in Fig. 4 and 5 for the chitosan/MPEG-*b*-PCL and chitosan/MPEG-*b*-PDLL nanocomposite films, respectively. From DTG thermograms, the temperature of maximum decomposition rate ($T_{d, max}$) can be determined and shown in Table 1. It was found that the chitosan, the MPEG-*b*-PCL and the MPEG-*b*-PDLL had a main $T_{d, max}$ at 296, 418 and 312°C, respectively.

The DTG thermograms of chitosan/MPEG-*b*-PCL nanocomposite films consisted of the both $T_{d, max}$ of chitosan and MPEG-*b*-PCL components. It should be noted that the both $T_{d, max}$ of each component of nanocomposite films slightly shift toward higher temperature than those of chitosan film and MPEG-*b*-PCL powder supporting intermolecular bonds existed between chitosan and MPEG-*b*-PCL nanoparticles. The results indicated that chitosan and the MPEG-*b*-PCL enhanced their thermal stability from intermolecular interaction according to chitosan/MPEG-*b*-PCL homogeneous blends (Noi *et al*., 2008).

However, the chitosan/MPEG-*b*-PDLL nanocomposite films showed only a single $T_{d, max}$ between the chitosan and the MPEG-*b*-PDLL in all composite ratios. The results supported that the smaller MPEG-*b*-PDLL nanoparticles are well dispersed into the chitosan film matrices.

Film transparency: The colors of chitosan and nanocomposite films were slight yellowish and whiteness tint, respectively. The film transparency was directly shown to their transmittances (%) at 660 nm (T_{660}) from UV-Vis spectrophotometry. The T_{660} values of films were shown in Table 2. The transparency of chitosan film was decreased when the nanoparticles were incorporated into the film matrices. As the increasing diblock copolymer ratios, the film transparency decreased. This may be due to the dispersed nanoparticles were opaque phases.

The chitosan/MPEG-*b*-PCL nanocomposite films showed more opaque than the chitosan/MPEG-*b*-PDLL nanocomposite films in all chitosan/diblock copolymer ratios. This could be explained that the MPEG-*b*-PCL chitosan and MPEG-*b*-PCL nanoparticles. The result

Table 1: Thermal decompositions of chitosan nanocomposite films and diblock copolymer powders

	$T_{d, max}$ (°C)	
Chitosan/diblock copolymer (w/w) nanocomposite films	Chitosan/MPEG-*b*-PCL film	Chitosan/MPEG-*b*-PDLL film
100/0	296	296
90/10	308, 429	299
80/20	309, 425	311
70/30	311, 423	317
0/100	418	322

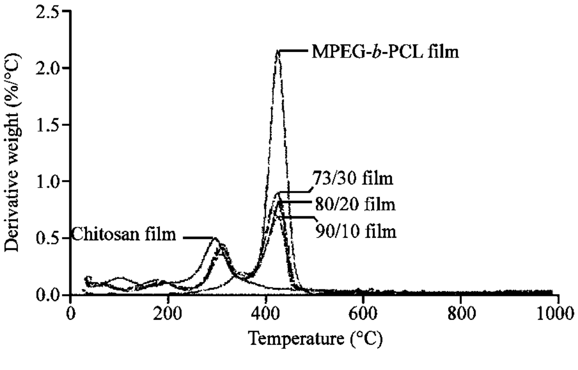

Fig. 4: DTG thermograms of chitosan, chitosan/MPEG-*b*-PCL nanocomposite and MPEG-*b*-PCL films

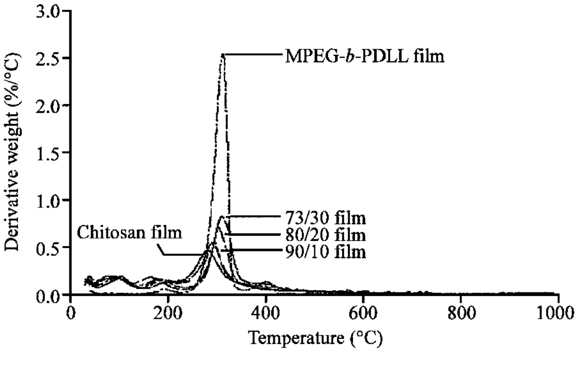

Fig. 5: DTG thermograms of chitosan, chitosan/MPEG-*b*-PDLL nanocomposite and MPEG-*b*-PDLL films

Table 2: Transparency and moisture uptakes of chitosan nanocomposite films

Chitosan/diblock copolymer (w/w) nanocomposite films	Transparency[a] (%T_{660})		Moisture uptake[a] (%)	
	Chitosan/MPEG-*b*-PCL film	Chitosan/MPEG-*b*-PDLL film	Chitosan/MPEG-*b*-PCL film	Chitosan/MPEG-*b*-PDLL film
100/0	78.7	78.7	79.5	79.5
90/10	37.2	72.5	79.0	79.3
80/20	29.2	71.3	78.5	79.0
70/30	27.2	70.6	78.0	78.8

[a]Measured from three samples and standard deviations less than 0.5

nanoparticles were larger in sizes and semi-crystalline phases, whereas the MPEG-*b*-PDLL nanoparticles were smaller in sizes and amorphous phases.

Moisture uptakes: The moisture (%) uptakes of chitosan and nanocomposite films were measured instead of water uptake (immersion in water) because of the partial dissolution of chitosan. The moisture (%) uptakes of films were calculated from Eq. 1 and also shown in Table 2. The moisture (%) uptake of the chitosan films was slightly decreased when the both MPEG-*b*-PCL and MPEG-*b*-PDLL nanoparticles were dispersed into the chitosan film suggested that the nanoparticles improved the moisture resistant of the chitosan film. The moisture uptakes (%) slightly decreased as the diblock copolymer ratio increased. This suggested that the hydrophobic characteristics of diblock copolymer exhibited resistant properties to water vapor.

However, the chitosan/MPEG-*b*-PCL nanocomposite films exhibited higher moisture resistant than the chitosan/MPEG-*b*-PDLL nanocomposite films in all chitosan/diblock copolymer ratios. This can be explained that the MPEG-*b*-PCL shows higher hydrophobicity than the MPEG-*b*-PDLL due to long chains of ethylene units in PCL blocks.

CONCLUSION

The chitosan nanocomposite films contained nanoparticles of diblock copolymers were successfully prepared by film casting of nanoparticle suspension-chitosan solution. The nanoparticles of MPEG-*b*-PCL or MPEG-*b*-PDLL diblock copolymers were formed. The MPEG-*b*-PCL nanoparticles sizes were smaller than the MPEG-*b*-PDLL. The nanopores were also observed throughout the chitosan film matrices. The incorporating MPEG-*b*-PCL nanoparticles into chitosan films enhanced thermal stability of the both chitosan film matrices and dispersed MPEG-*b*-PCL nanoparticles, whereas thermal stability of only chitosan film matrices were improved when the MPEG-*b*-PDLL was used instead of MEPG-*b*-PCL. The film transparency and moisture uptakes of chitosan films decreased as the nanoparticles incorporated. These nanocomposite films might be of interested for use in biomedical, pharmaceutical and packaging applications.

ACKNOWLEDGMENT

This research was supported by the Center of Excellence for Innovation in Chemistry (PERCH-CIC), Commission on Higher Education, Ministry of Education, Thailand.

REFERENCES

Baimark, Y., M. Srisa-ard, J. Threeprom, R. Molloy and W. Punyodom, 2007a. Synthesis and characterization of metoxy poly (ethylene glycol)-b-poly (Dl-lactide-co-glycolide-co-Î Punyodom, 2007. Synthesis and characterization of methoxy poly (ethylene glycol)-b-poly (Dl-lactide-co-glycolide-co-Îμ-caprolactone) diblock copolymers: Effects of block lengths and compositions. e-Polymers, 138: 1-9.

Baimark, Y., N. Niamsa, N. Morakot, J. Threeprom and Y. Srisuwan, 2007b. Preparation and morphology study of biodegradable chitosan/methoxy poly (ethylene glycol)-b-poly (ϵ-caprolactone) nanocomposite films. Int. J. Polym. Anal. Charat., 12: 457-467.

Chen, C., L. Dong and M.K. Cheung, 2005. Preparation and characterization of biodegradable poly (L-lactide)/chitosan blends. Eur. Polym. J., 41: 958-966.

Khamhan, S., Y. Baimark, S. Chaichanadee, P. Phinyocheep and S. Kittipoom, 2008. Water vapor permeability and mechanical properties of biodegradable chitosan/ methoxy poly (ethylene glycol)-*b*-poly(ϵ-caprolactone) nanocomposite films. Int. J. Polym. Anal. Cha., 13: 224-231.

Muzzarelli, R.A.A. and C. Muzzarelli, 2005. Chitosan chemistry: Relevance to the biomedical sciences. Adv. Polym. Sci., 186: 151-209.

Noi, N., A. Puntumchai, V. Sutthikhum, Y. Srisuwan and Y. Baimark, 2008. Preparation and characterization of biodegradable chitosan and methoxy poly(ethylene glycol)-b-poly (ϵ-caprolactone) blend homogeneous films. J. Applied Polymer Sci., 109: 418-423.

Park, S.I. and Y. Zhao, 2004. Incorporation of a high concentration of mineral or vitamin into chitosan-based films. J. Agric. Food Chem., 52: 1933-1939.

Perugini, P., I. Genta, B. Conti, T. Modena and F. Pavanetto, 2003. Periodontal delivery of ipriflavone: New chitosan/PLGA film delivery system for a lipophilic drug. Int. J. Pharm., 252: 1-9.

Ravi-Kumaer, M.N.V., R.A.A. Muzzarelli, C. Muzzarelli, H. Sashiwa and A.J. Domb, 2004. Chitosan chemistry and pharmaceutical perspective. Chem. Rev., 104: 6017-6084.

Rhim, J.W., S.I. Hong, H.M. Park and P.K.W. Ng, 2006. Preparation and characterization of chitosan-based nanocomposite films with antimicrobial activity. J. Agric. Food Chem., 54: 5814-5822.

Senel, S., G. Ikinci, S. Kas, A. Yousefi-Rad, M.F. Sargon and A.A. Hincal, 2000. Chitosan films and hydrogel of chlorhexidine gluconate for oral mucosal delivery. Int. J. Pharm., 193: 197-203.

Shu, X.Z., K.J. Zhu and W. Song, 2001. Novel pH-sensitive citrate cross-linked chitosan film for drug controlled release. Int. J. Pharm., 212: 19-28.

Zhang, M., X.H. Li, Y.D. Gong, N.M. Zhao and X.F. Zhang, 2002. Properties and biocompatibility of chitosan films modified by blending with PEG. Biomaterials, 23: 2641-2648.